Supporting Information

Electrocatalytic hydrogen evolution reaction of cobalt triaryl corrole bearing nitro group

Jie Zeng [1], Xu-You Cao [1], Shi-Yin Xu [1], Yi-Feng Qiu [1], Jun-Ying Chen [1,*], Li-Ping Si [1, 2*] and Hai-Yang Liu [1,*]

1 Guangdong Provincial Key Laboratory of Fuel Cell Technology, School of Chemistry and Chemical Engineering, South China University of Technology, Guangzhou 510641, China

2 School of Materials Science and Energy, Foshan University, Foshan 528000, China

* Correspondence: lipingsi@fosu.edu.cn (L.-P.S.); cejychen@scut.edu.cn (J.-Y .C.); chhyliu@scut.edu.cn (H.-Y .L.)

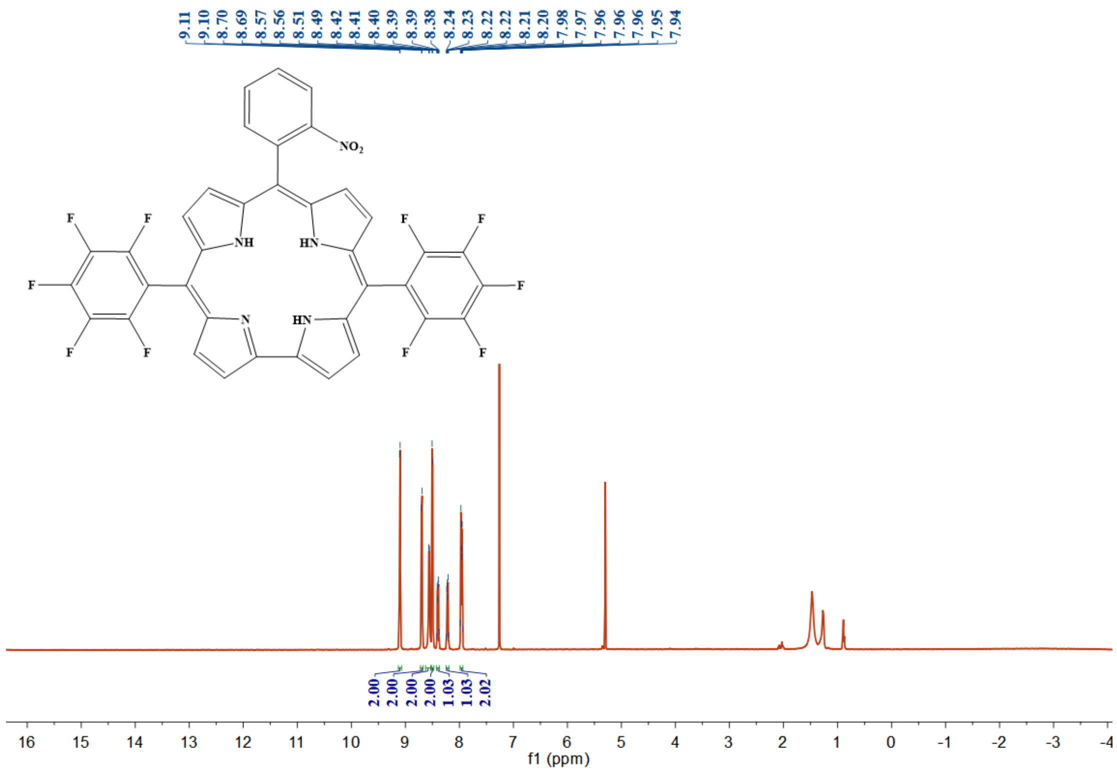

Figure S1. ^{1}H NMR spectrum of 2-NBPC.

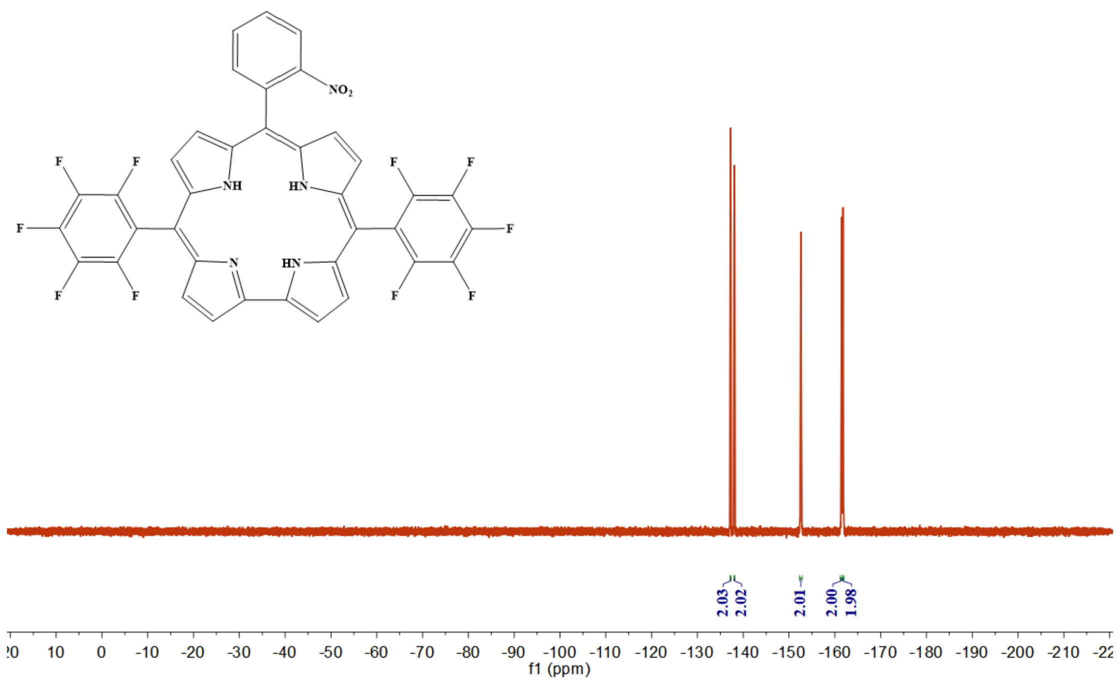

Figure S2. ^{19}F NMR spectrum of 2-NBPC.

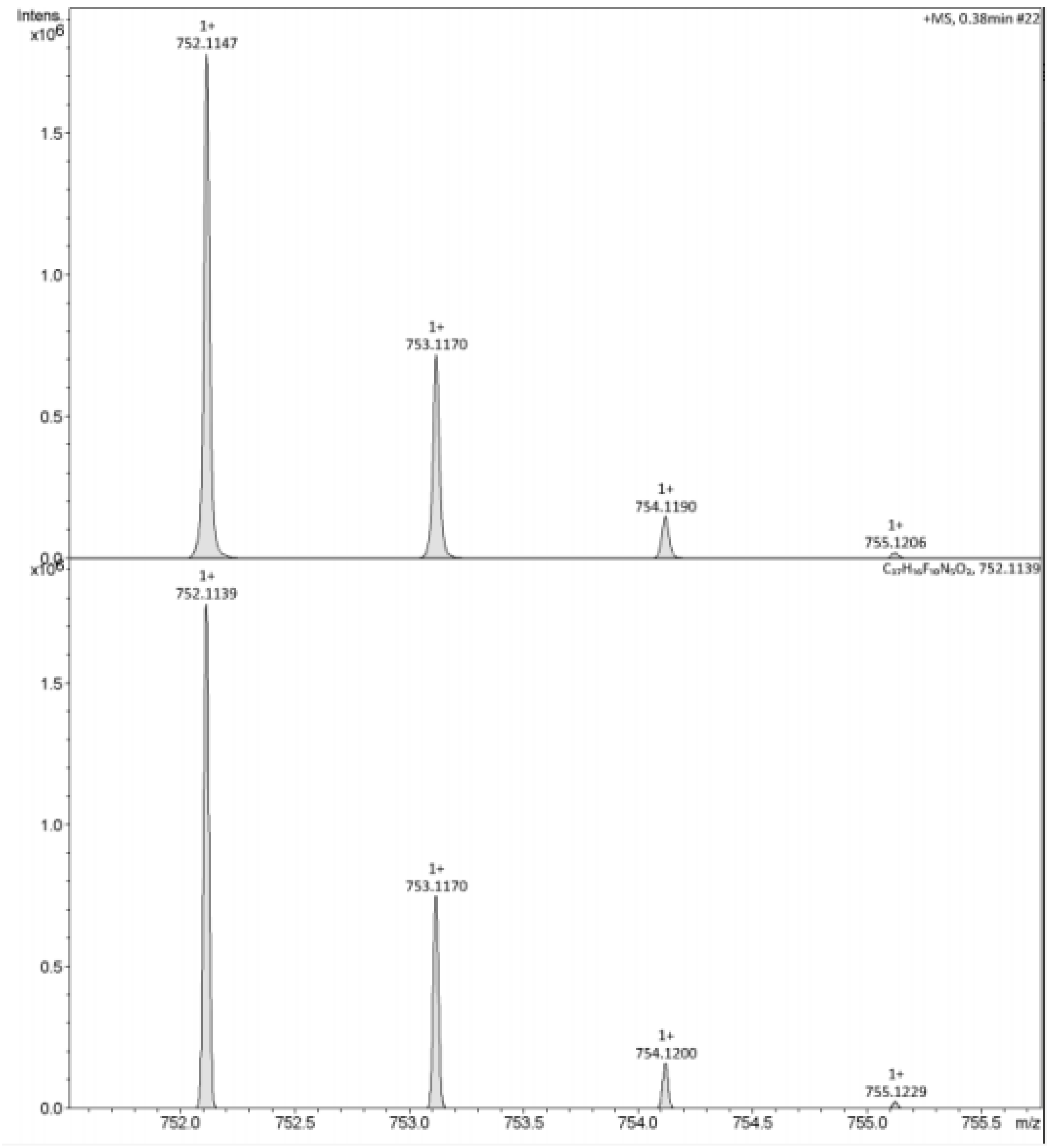

Figure S3. ESI-HRMS spectrum of 2-NBPC.

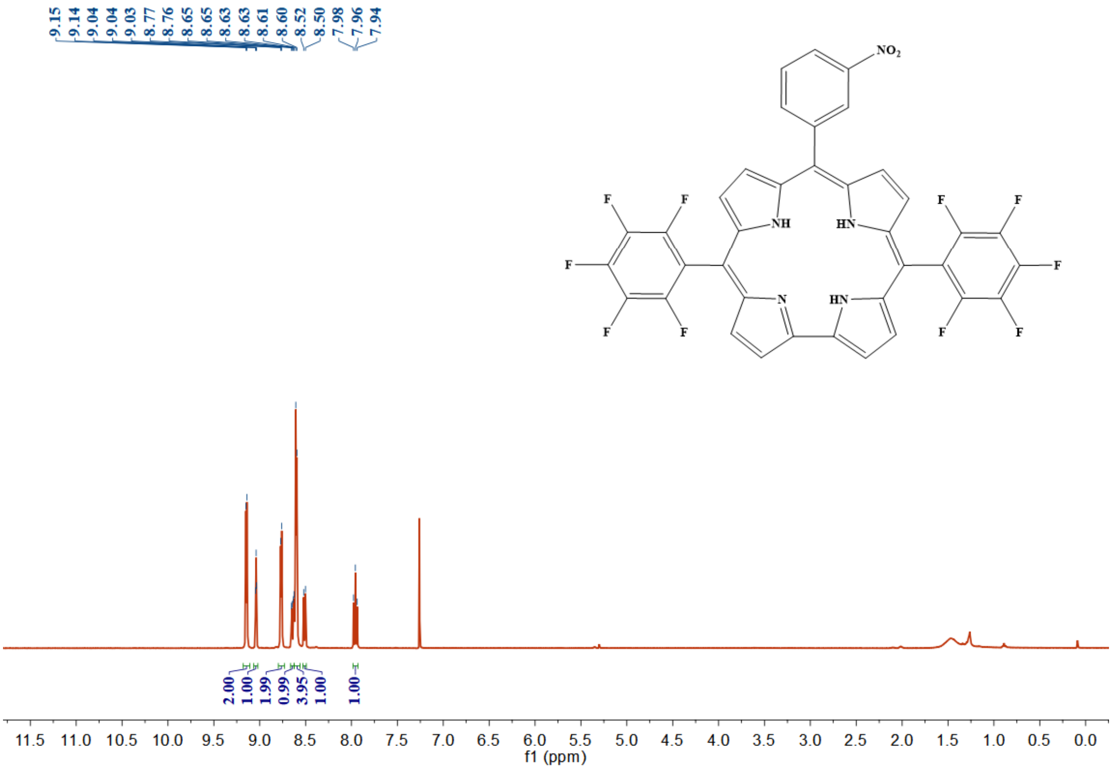

Figure S4. ^{1}H NMR spectrum of 3-NBPC.

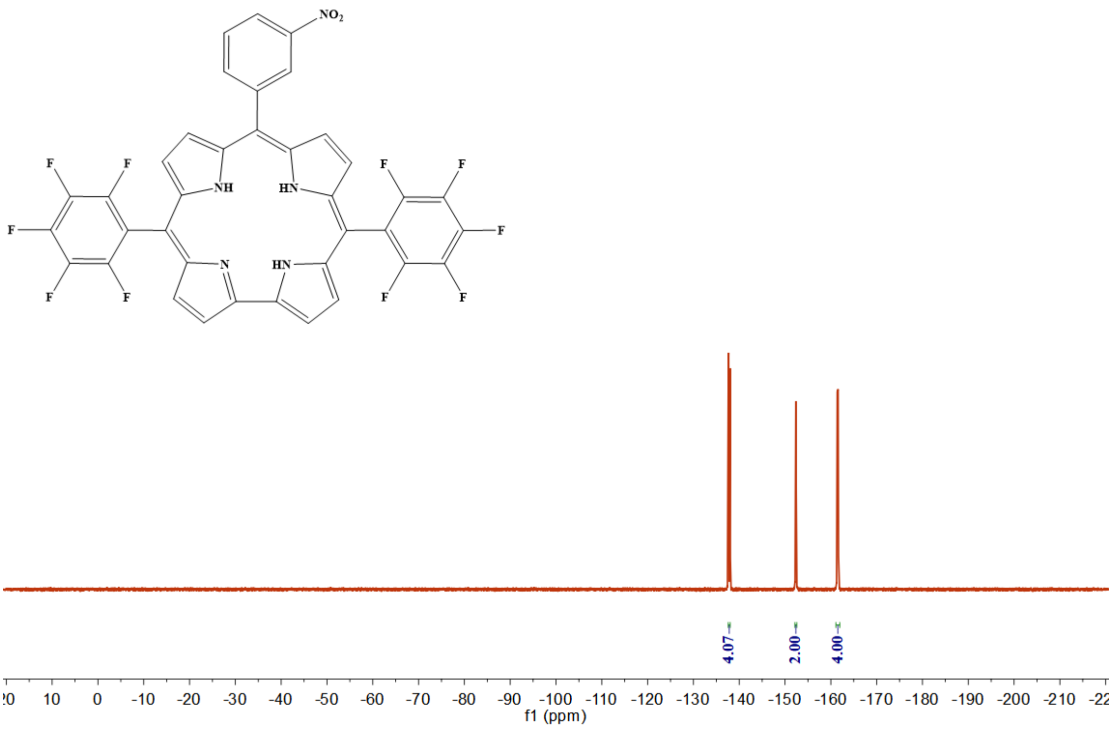

Figure S5. ^{19}F NMR spectrum of 3-NBPC.

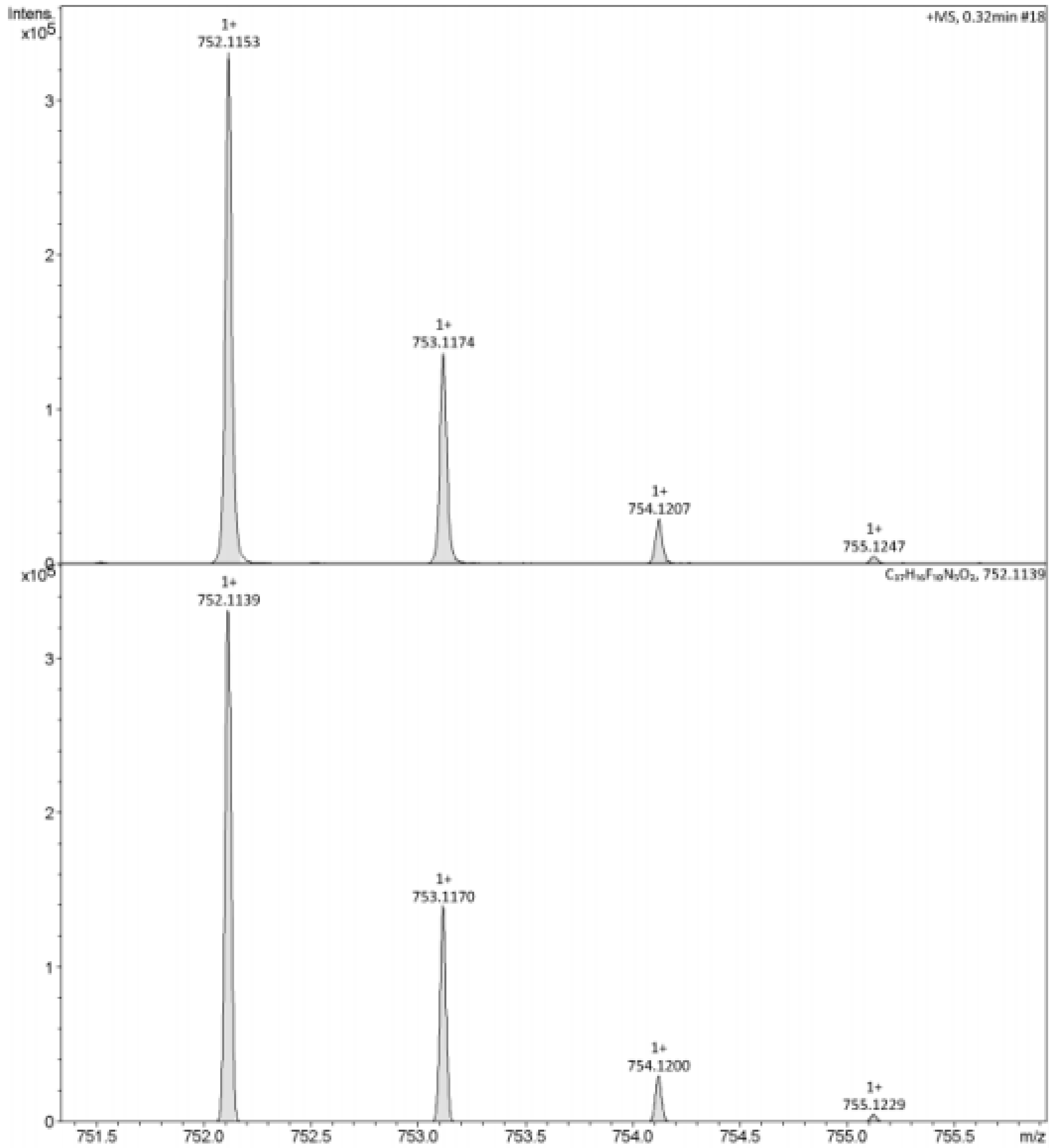

Figure S6. ESI-HRMS spectrum of 3-NBPC.

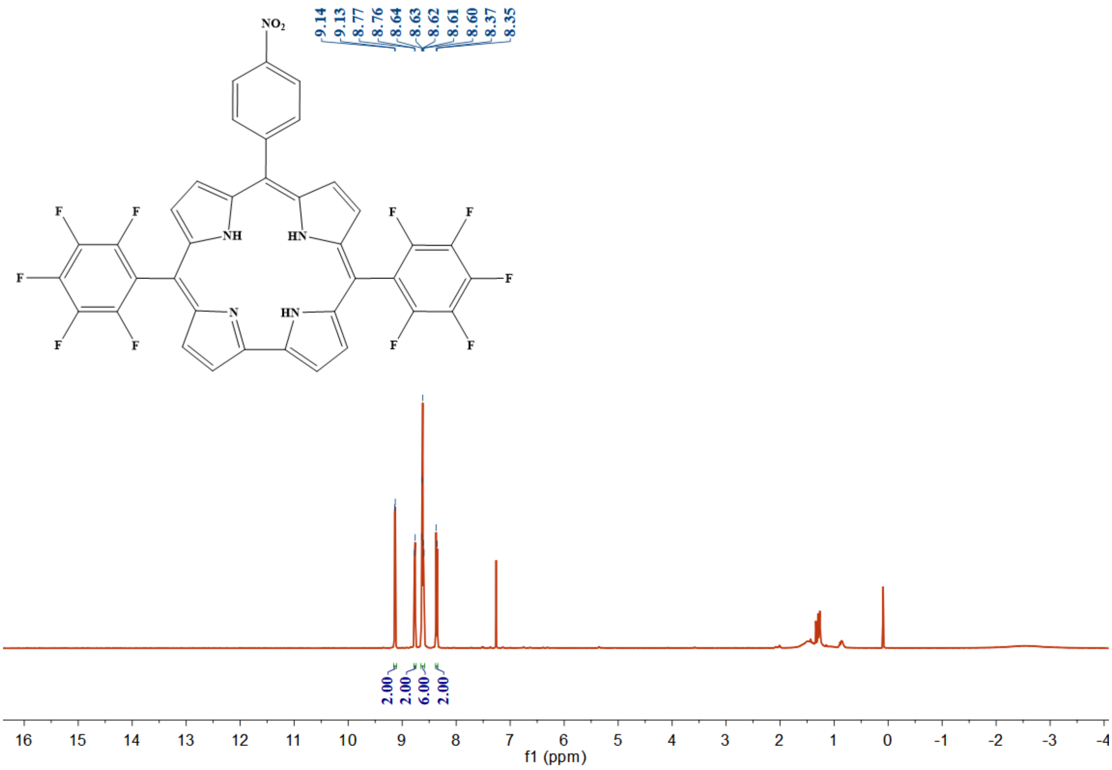

Figure S7. ^{1}H NMR spectrum of 4-NBPC.

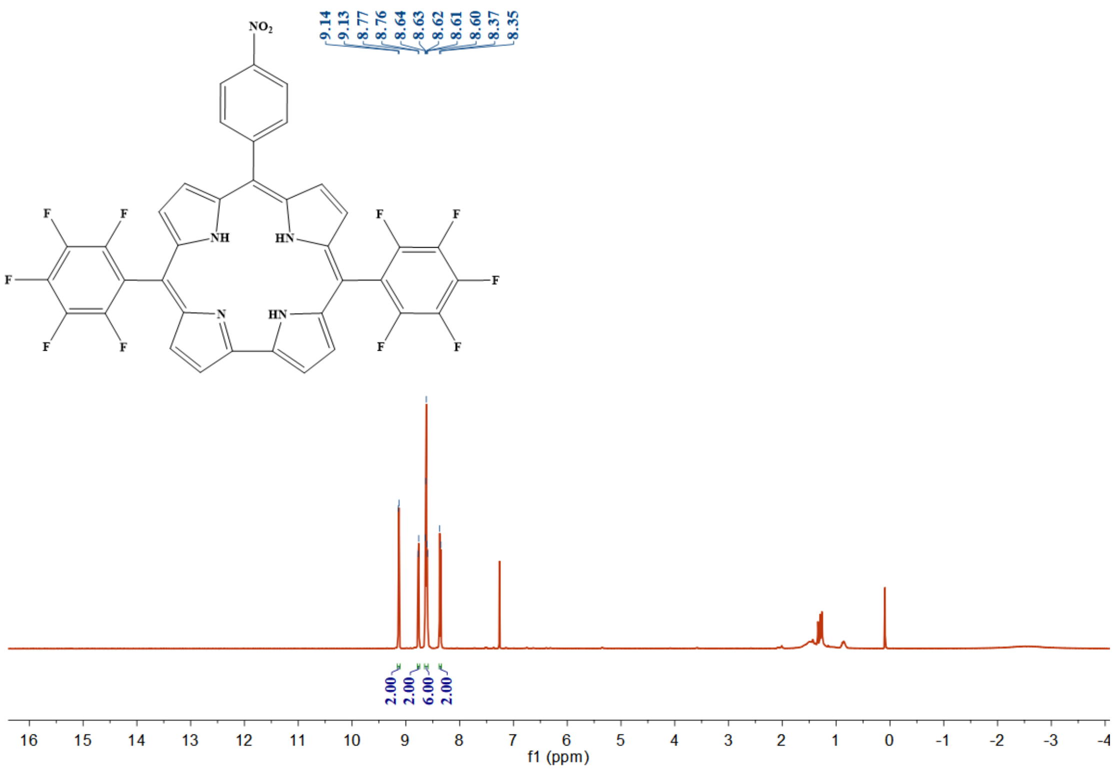

Figure S8. ^{19}F NMR spectrum of 4-NBPC.

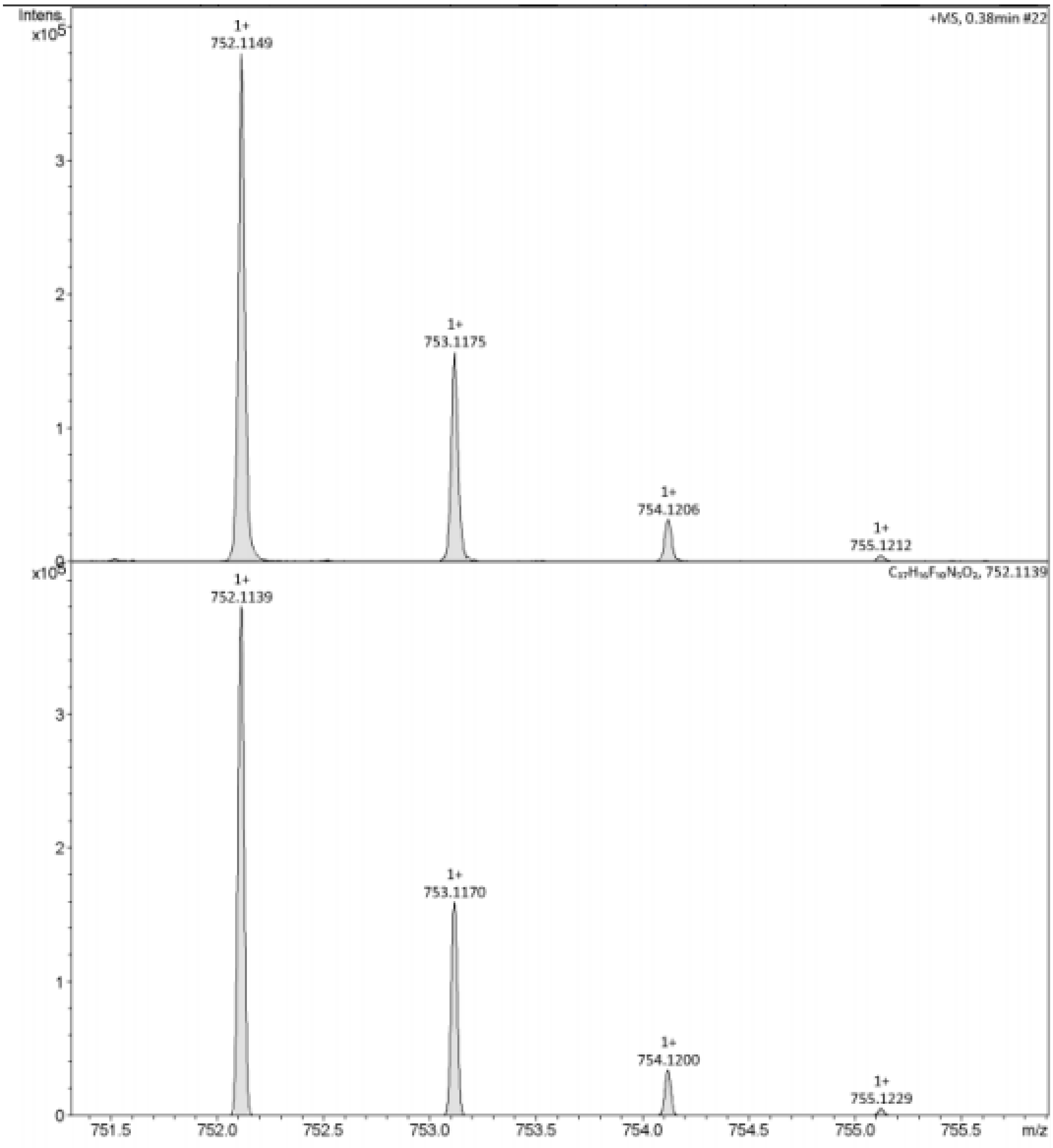

Figure S9. ESI-HRMS spectrum of 4-NBPC.

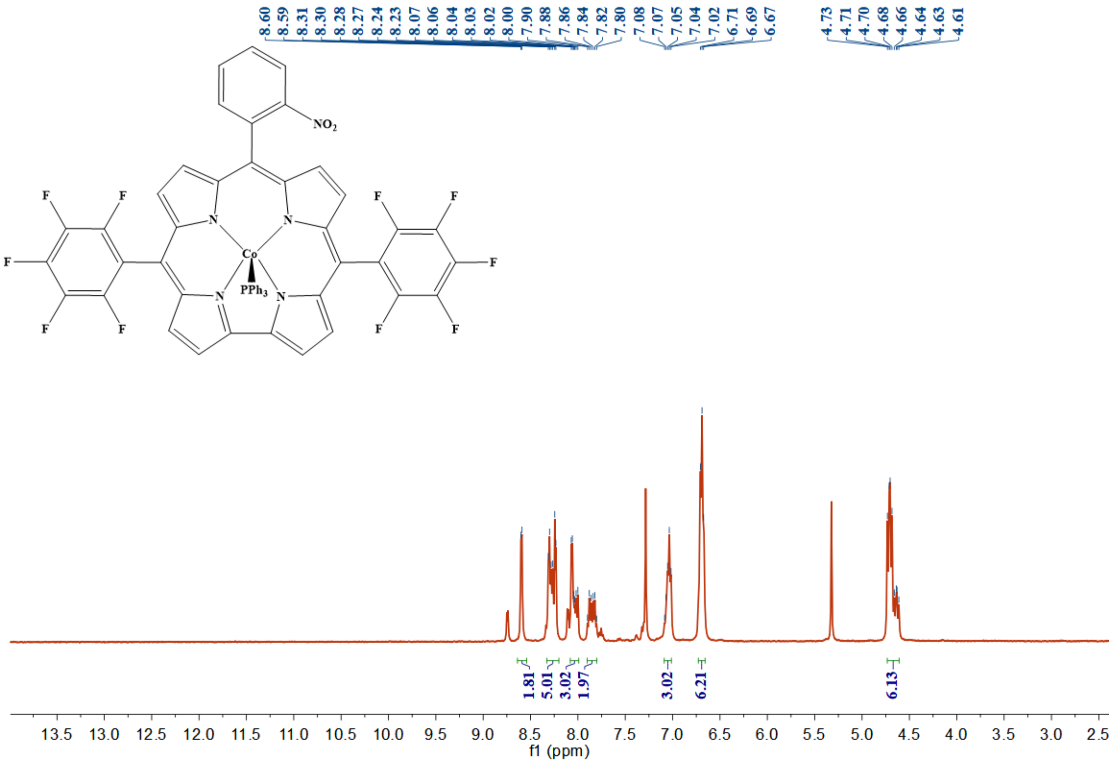

Figure S10. ^{1}H NMR spectrum of Complex **1**.

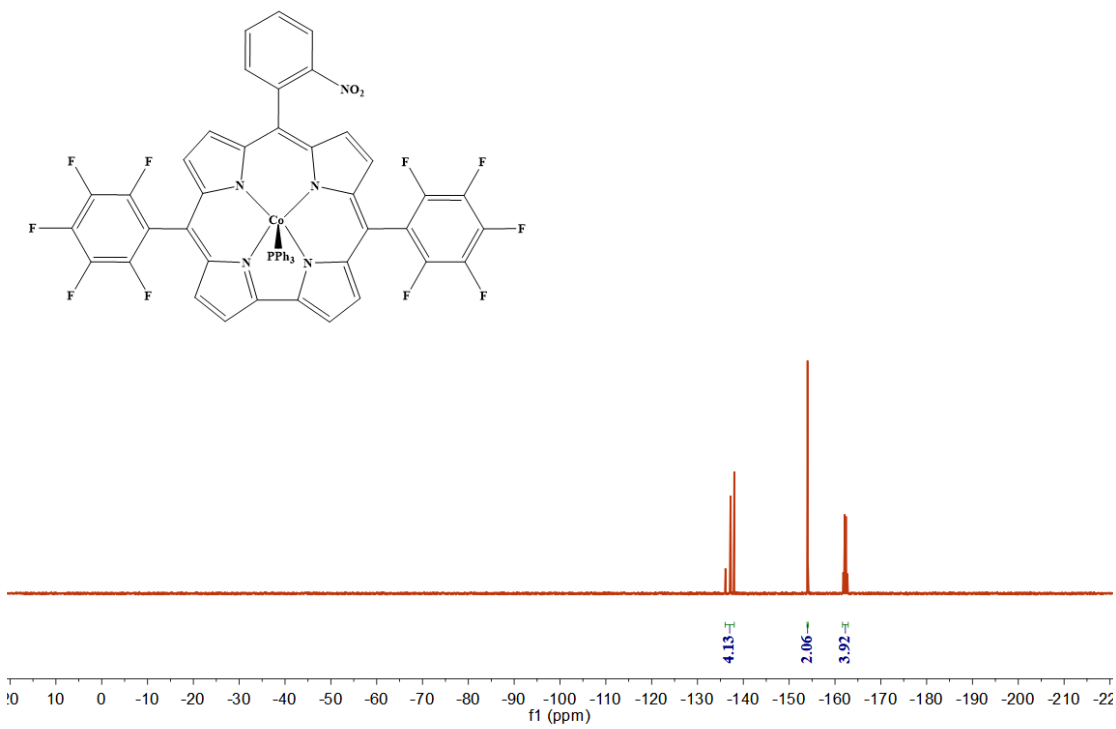

Figure S11. ^{19}F NMR spectrum of Complex **1**.

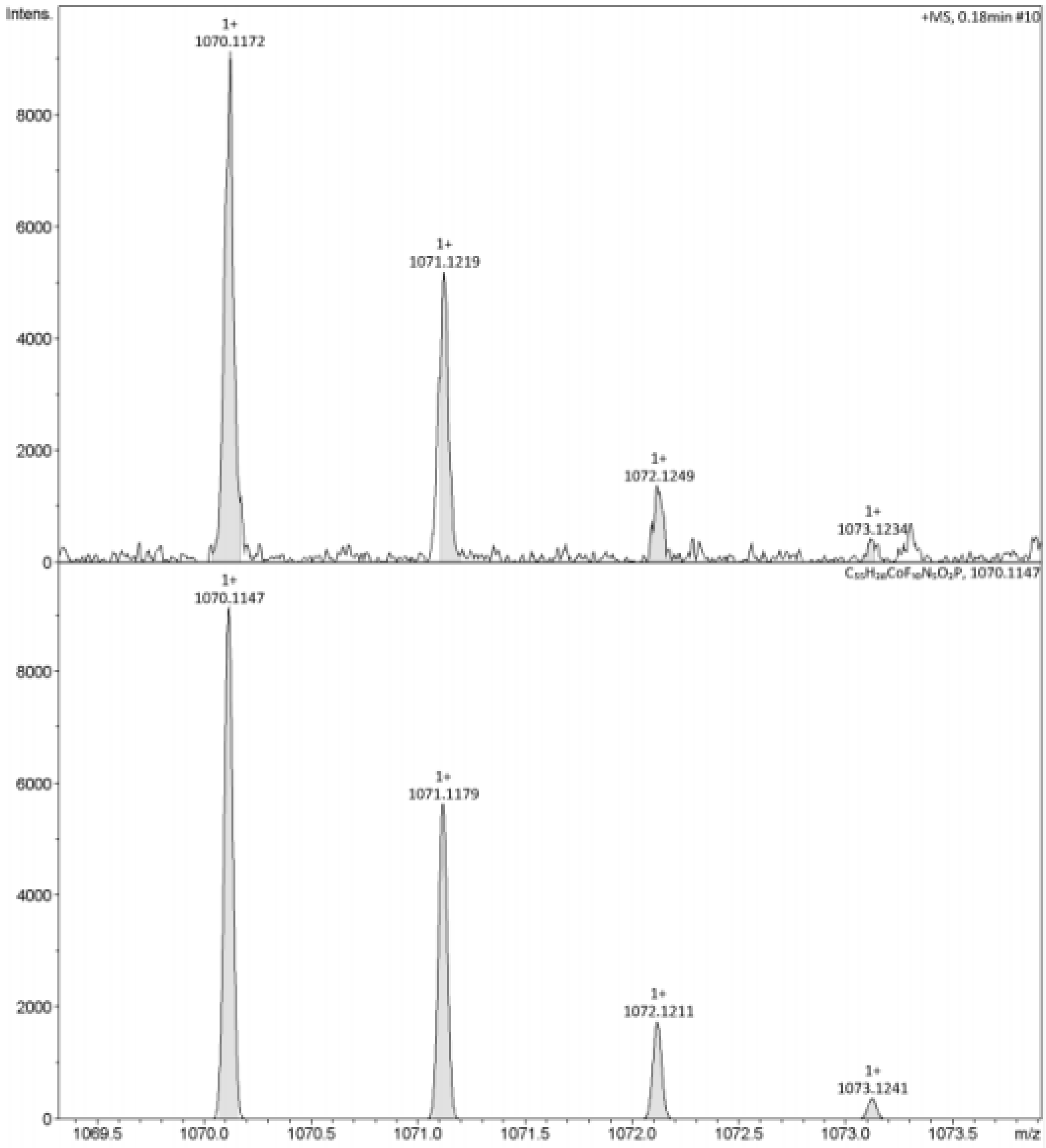

Figure S12. ESI-HRMS spectrum of Complex **1**.

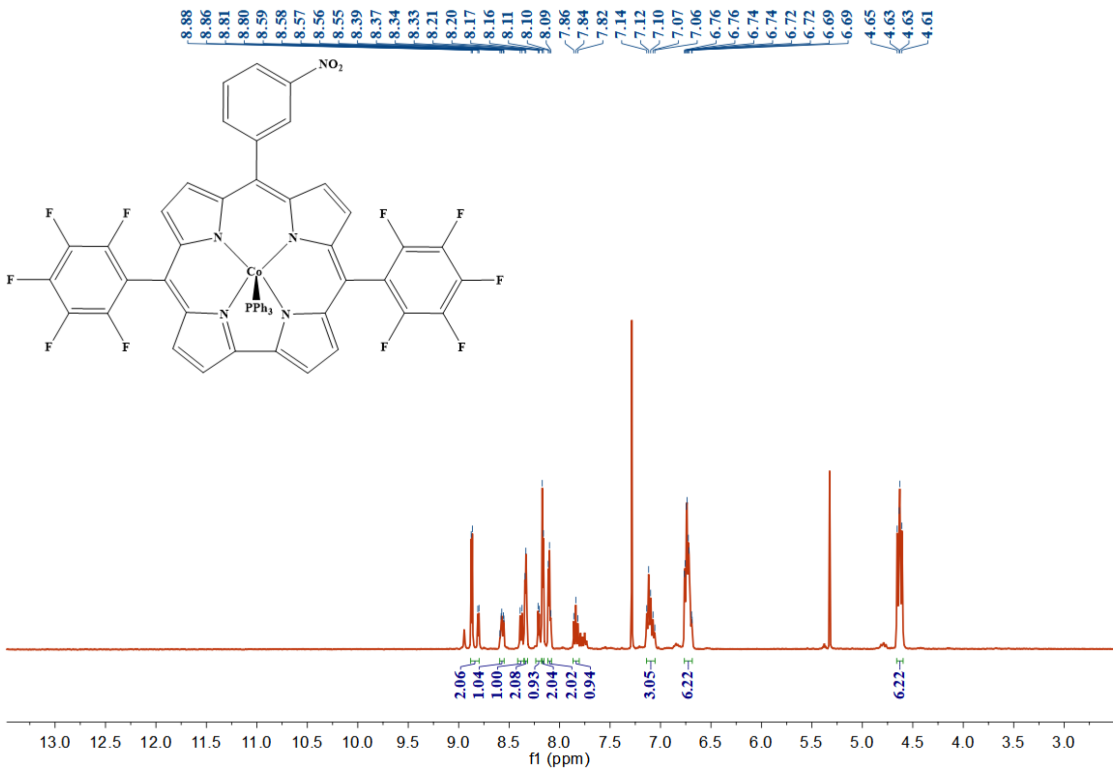

Figure S13. ^{1}H NMR spectrum of Complex **2**.

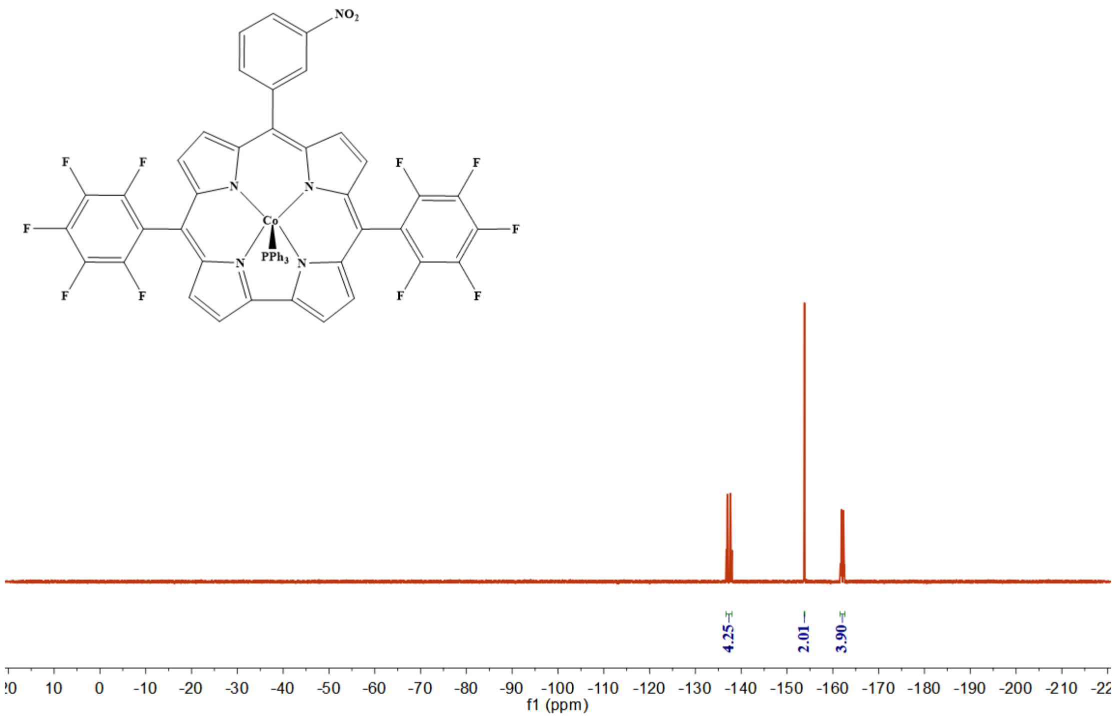

Figure S14. ^{19}F NMR spectrum of Complex **2**.

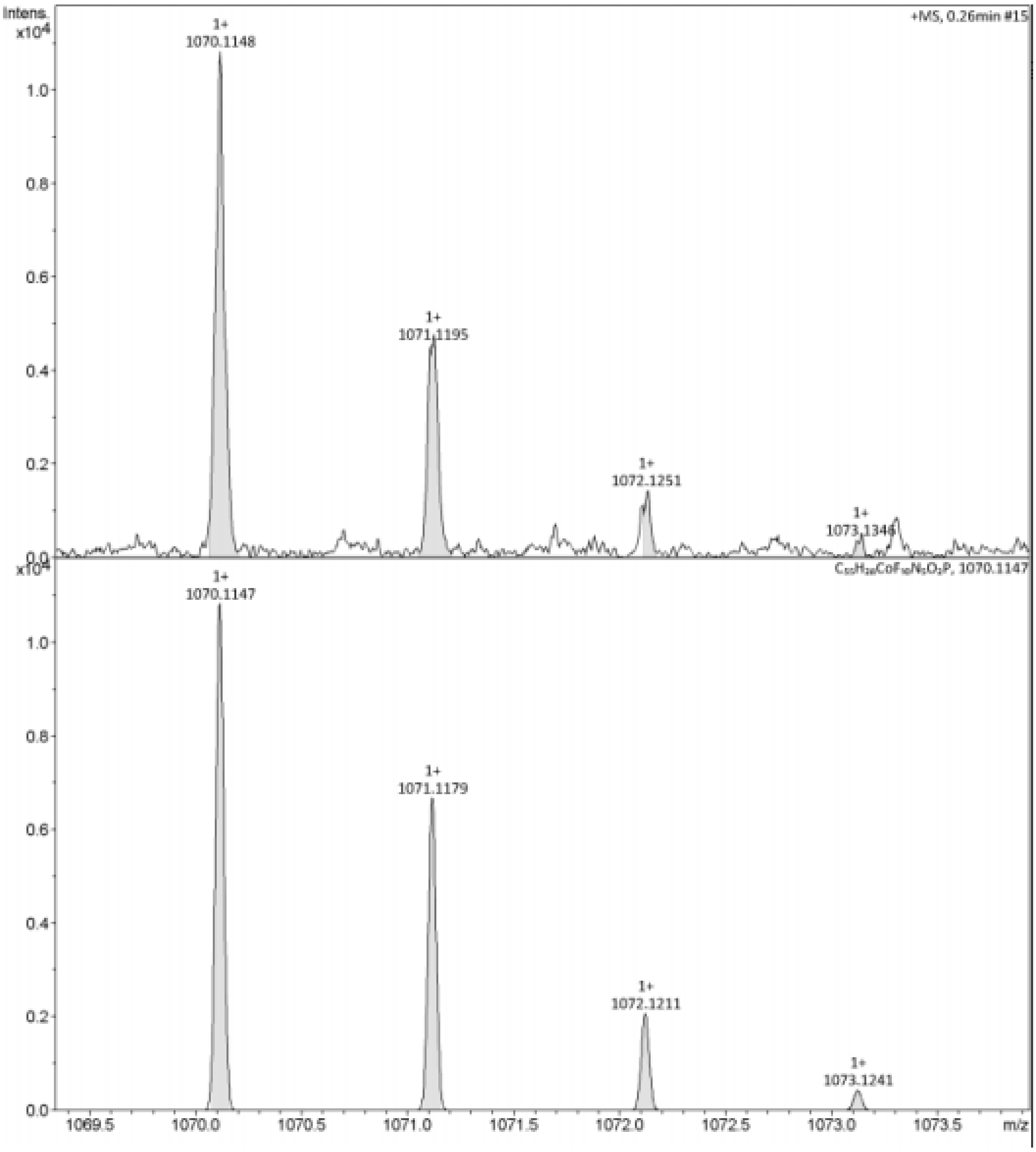

Figure S15. ESI-HRMS spectrum of Complex **2**.

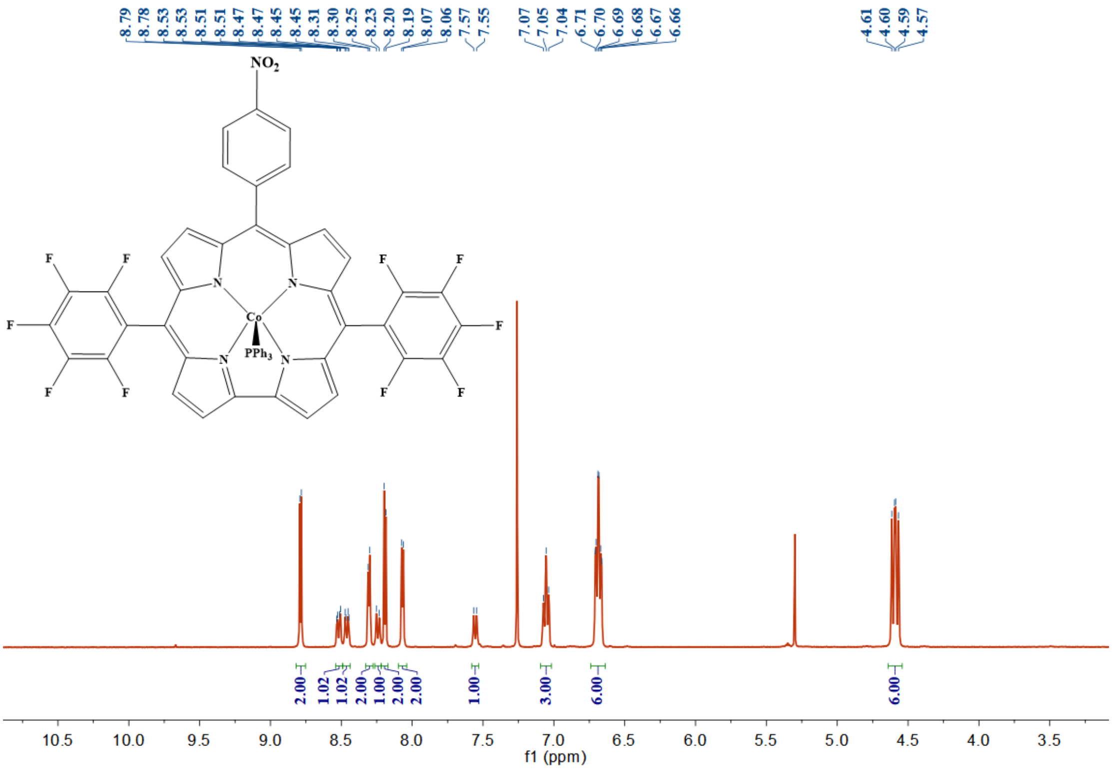

Figure S16. ^{1}H NMR spectrum of Complex **3**.

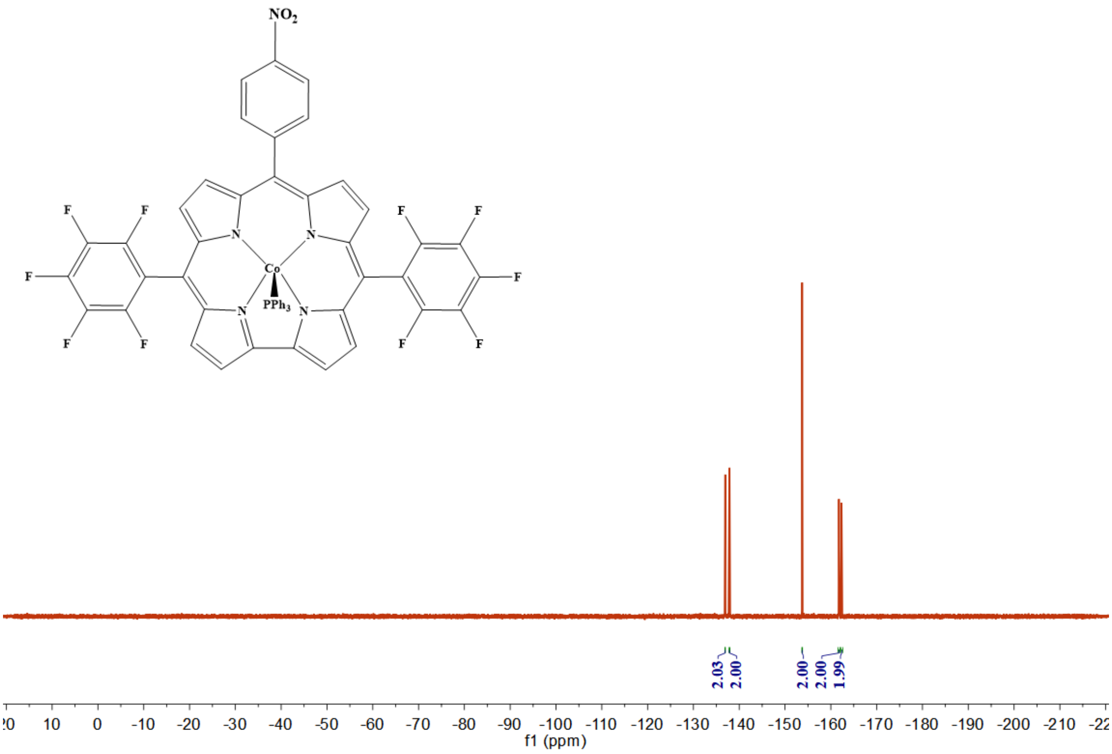

Figure S17. ^{19}F NMR spectrum of Complex **3**.

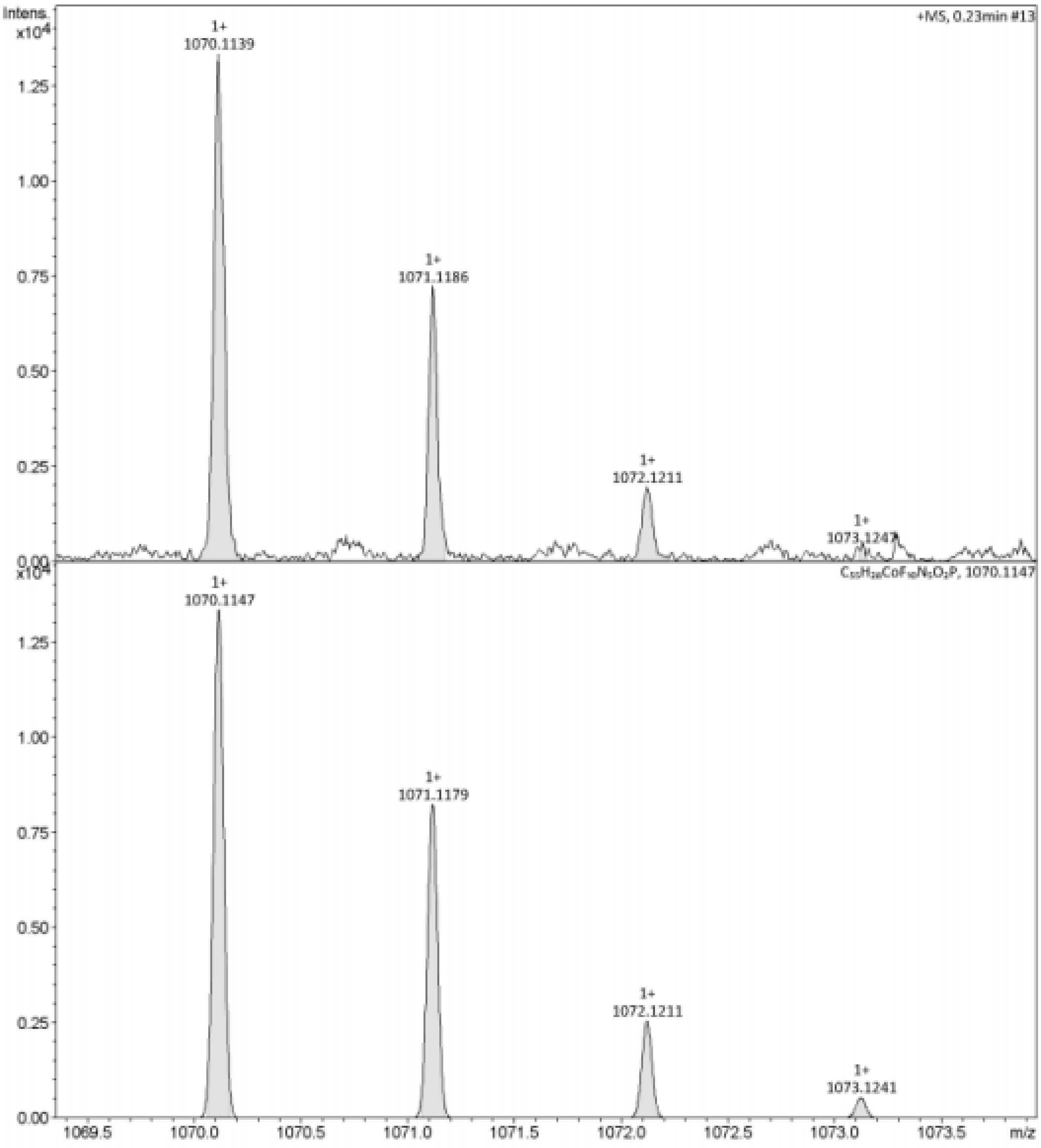

Figure S18. ESI-HRMS spectrum of Complex **3**.

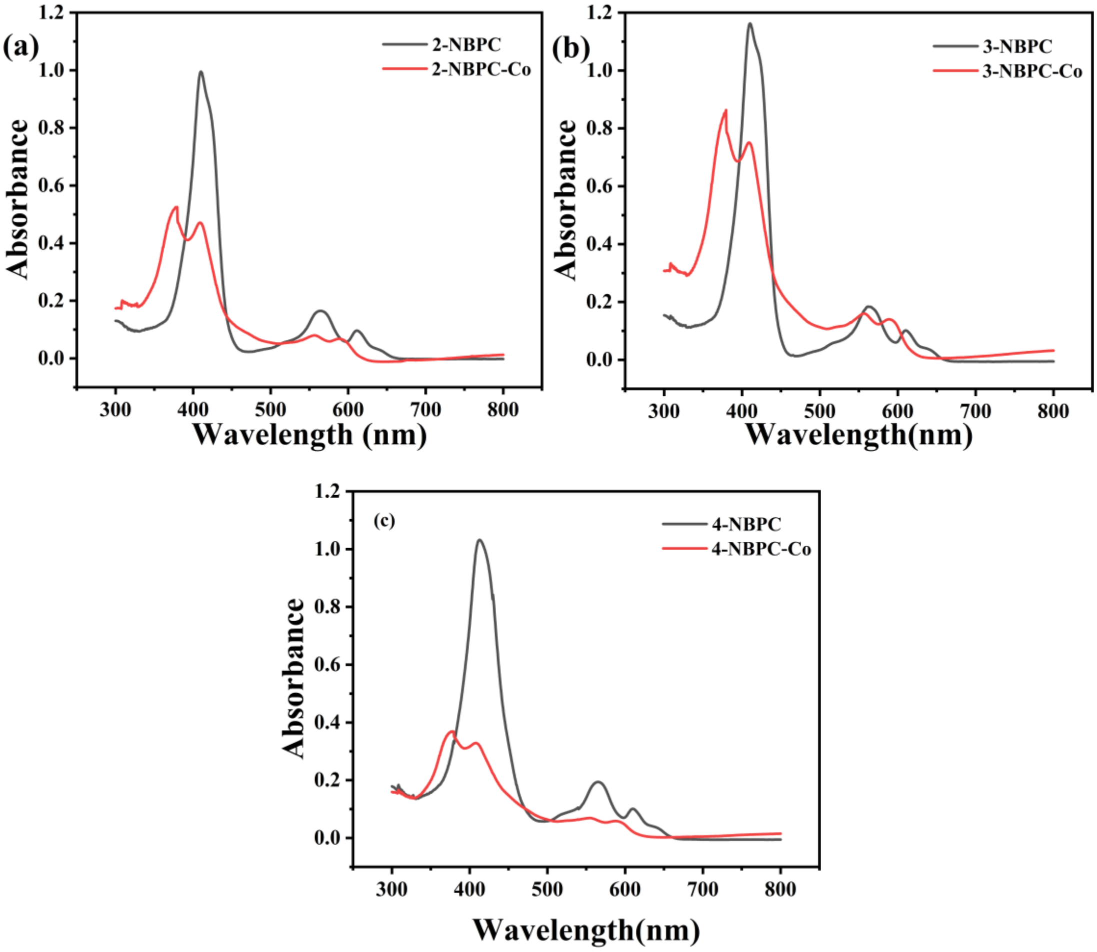

Figure S19. UV-Vis spectra of 2-NBPC and 2-NBPC-Co (**1**) (**a**), 3-NBPC and 3-NBPC-Co (**2**) (**b**), 4-NBPC and 4-NBPC-Co (**3**) (**c**) in DCM.

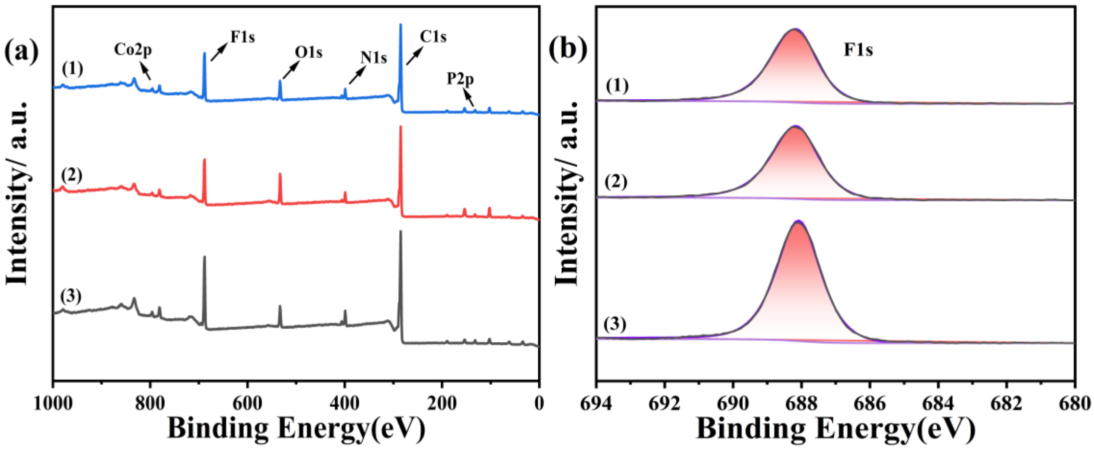

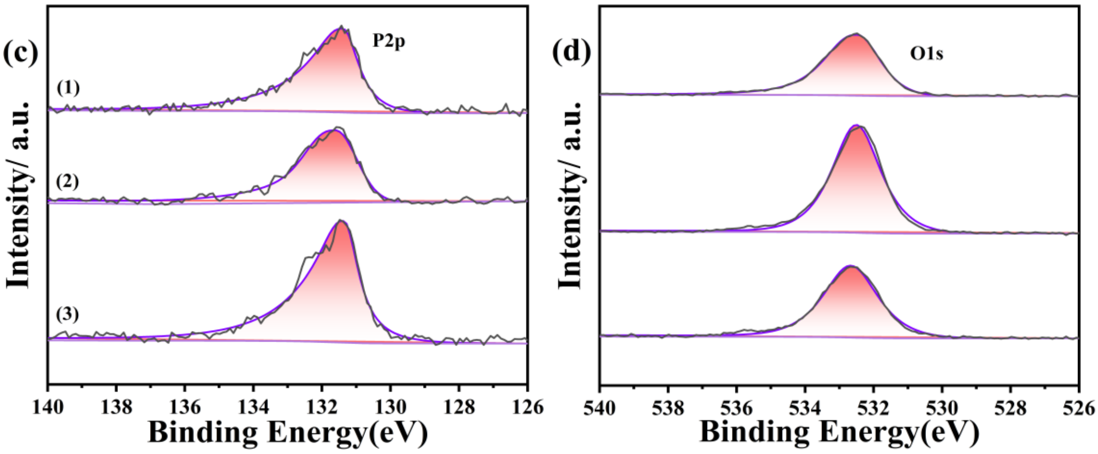

Figure S20. XPS survey spectrum (**a**); XPS spectra of F 1s (**b**) and P 2p (**c**) and O 1s (**d**) of complexes **1**-**3**.

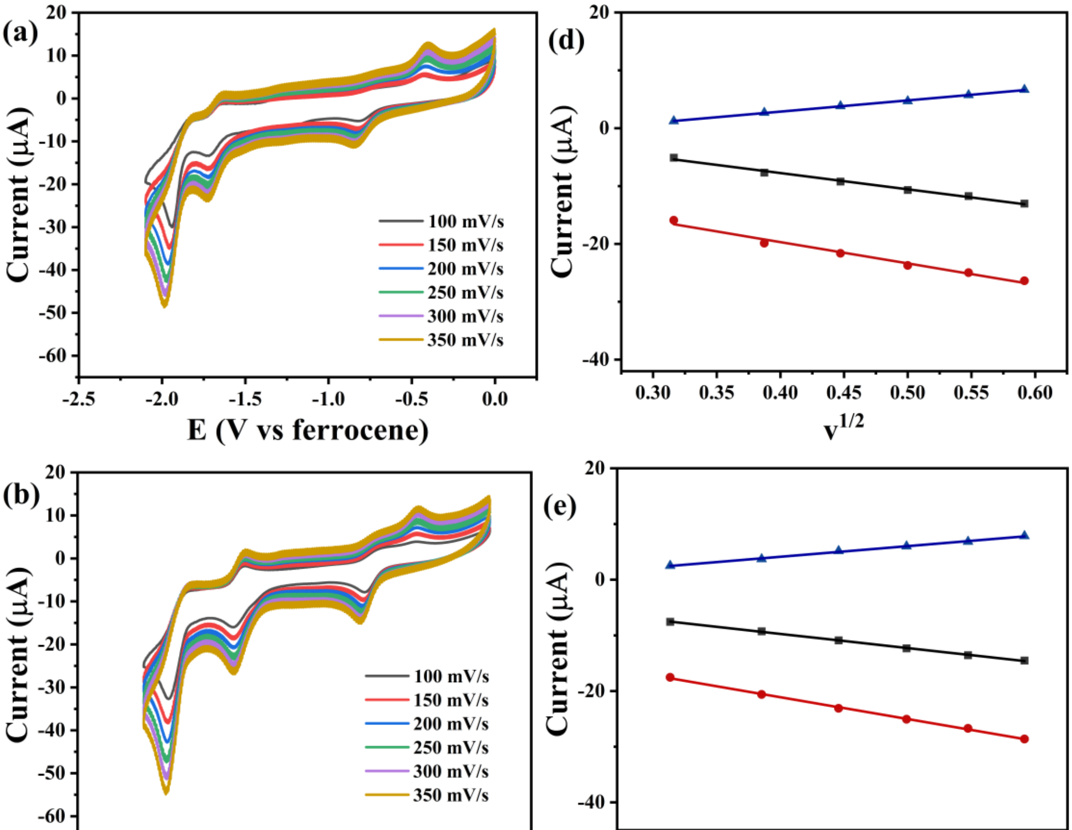

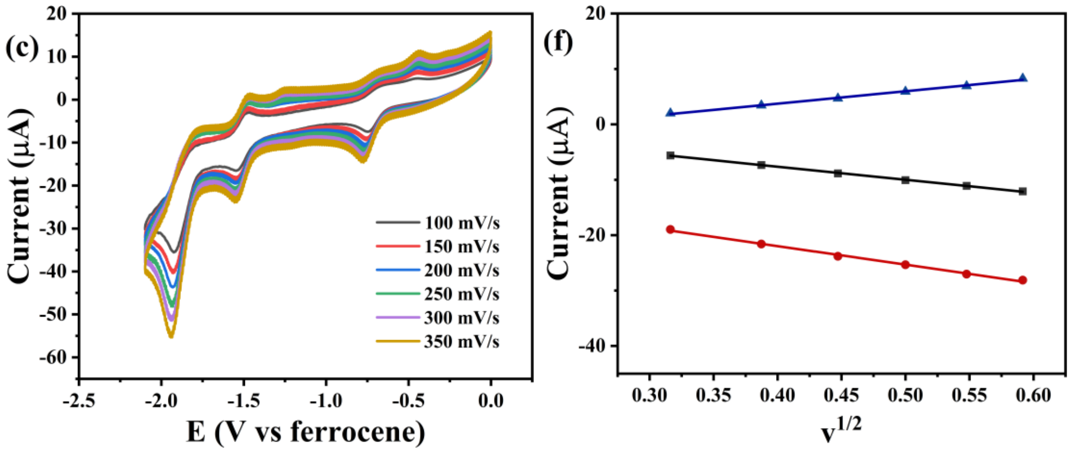

Figure S21. CVs of 0.5 mM complexes **1** (**a**), **2** (**b**) and **3** (**c**) in a varying scan rate (v) from 100 mV/s to 350 mV/s; Plot of peak current (i_p) values of complexes **1** (**d**), **2** (**e**), **3** (**f**) versus the square root of the scan rate ($v^{1/2}$).

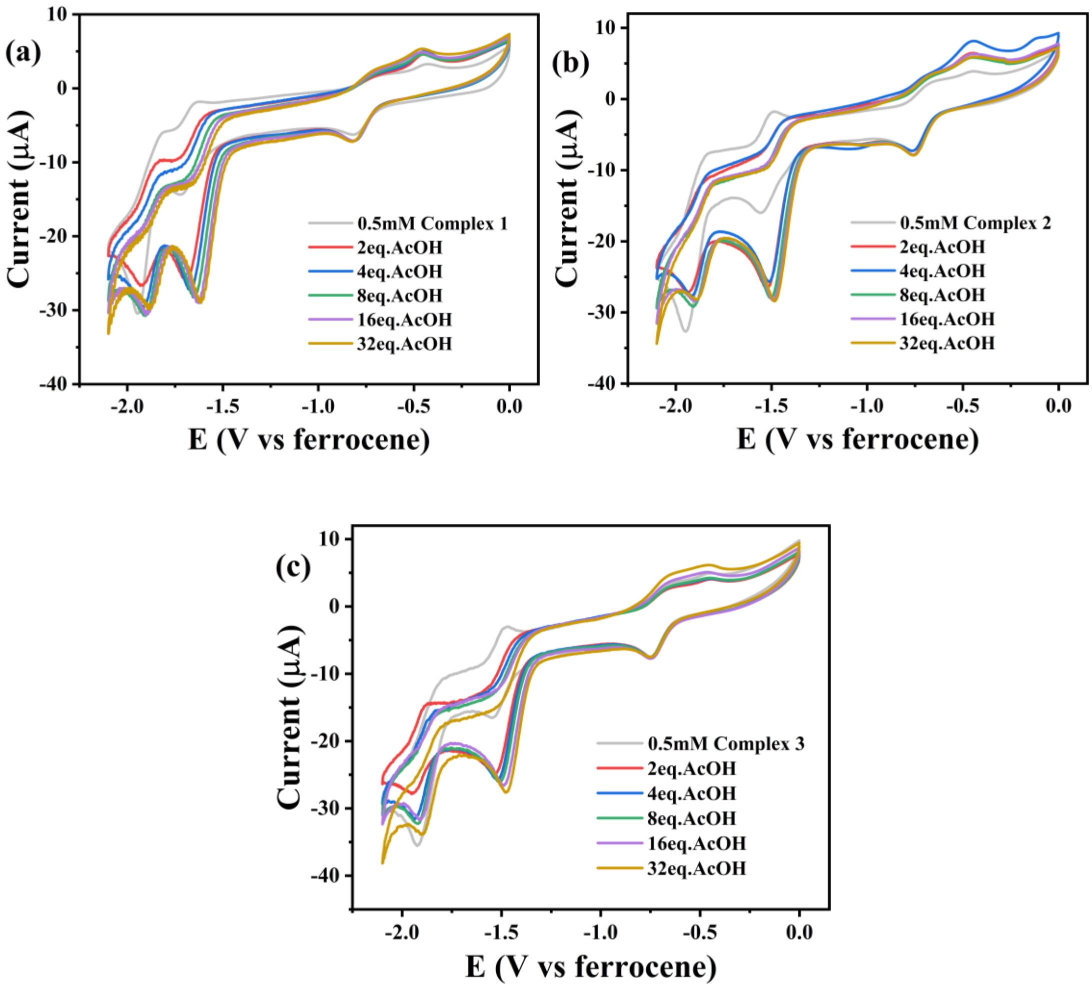

Figure S22. CVs of 0.5 mM complexes **1** (**a**), **2** (**b**), and **3** (**c**) in DMF (0.1 M TBAP).

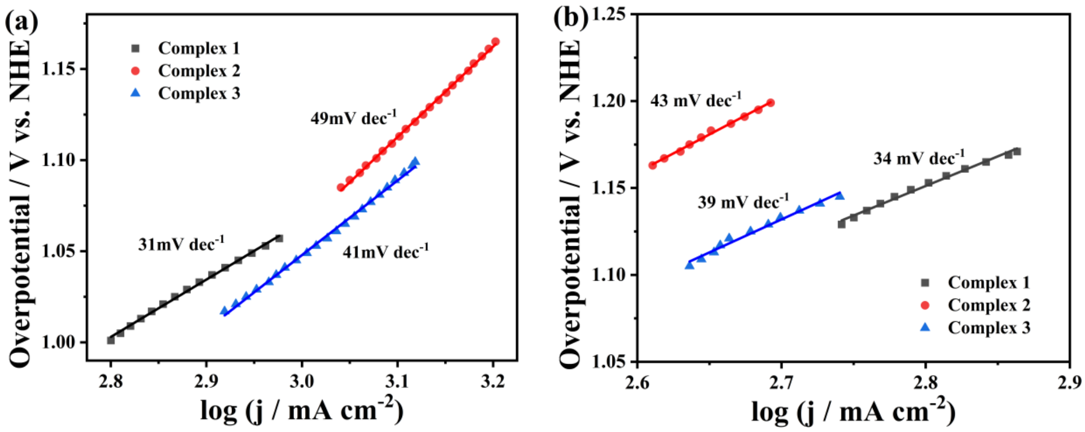

Figure S23. Tafel plots of the 0.5 mM complexes **1**-**3** with 32 eq. TFA (**a**), and 32 eq. TsOH (**b**) in DMF.

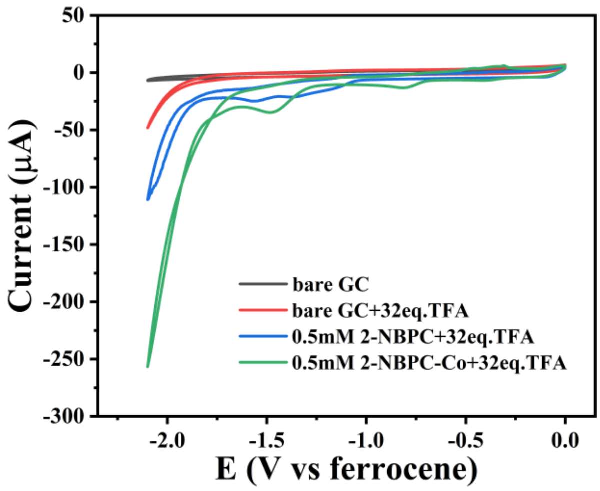

Figure S24. CVs of bare glassy carbon electrode without TFA (black), bare glass carbon electrode (red), 0.5 mM 2-NBPC (blue), and 0.5 mM 2-NBPC-Co (**1**)(green) with 32 eq. TFA in DMF.

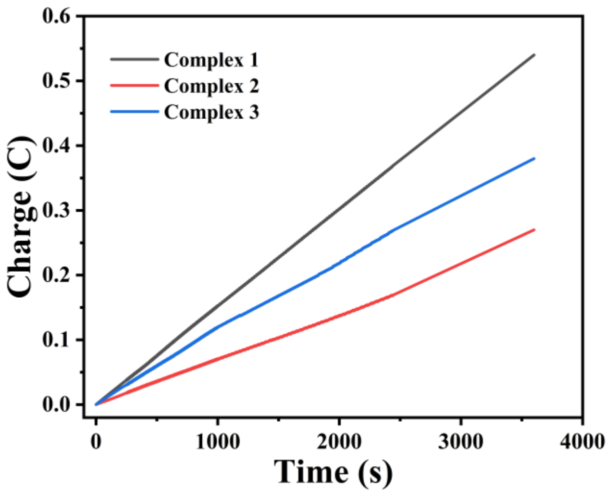

Figure S25. Charge of 0.5 mM complexes **1**, **2** and **3** after 1 h of electrolysis in DMF with excessive TFA.

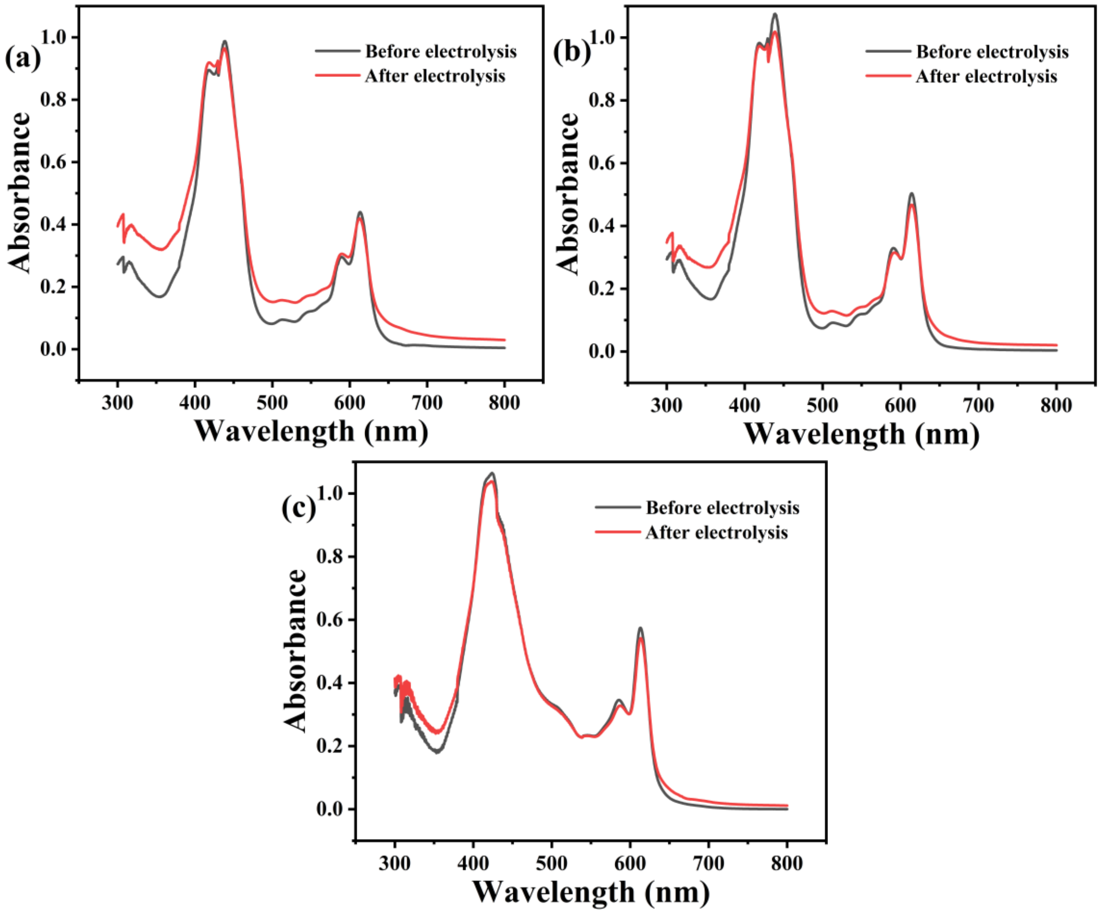

Figure S26. UV-vis of complexes **1** (**a**), **2** (**b**) and **3** (**c**) before and after 1 h of electrolysis in excessive TFA.

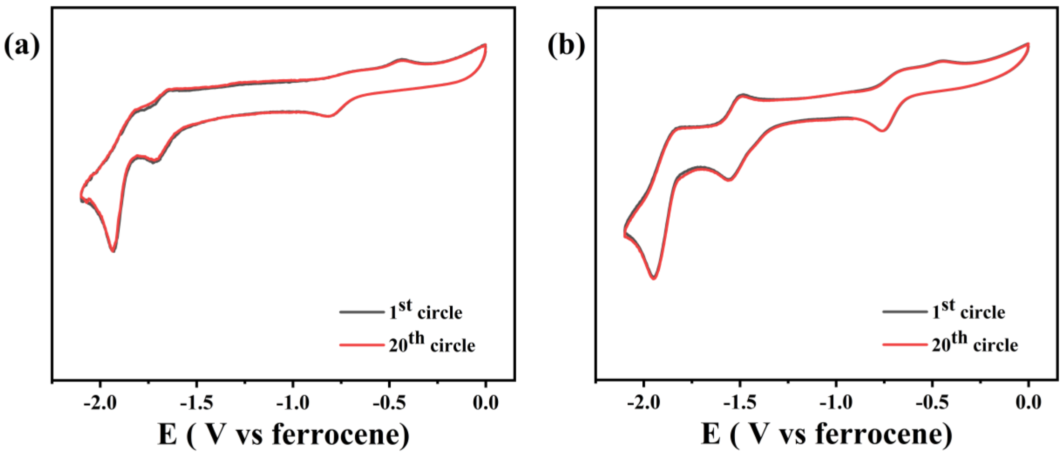

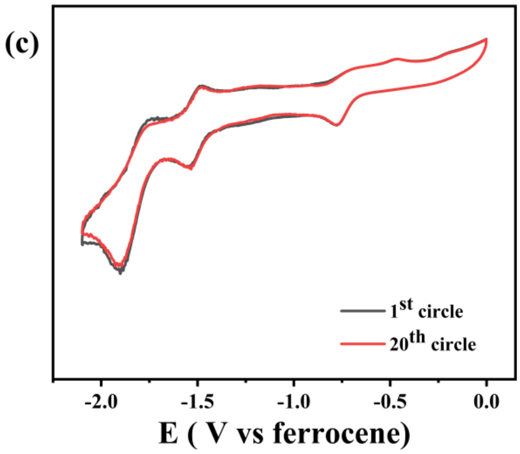

Figure S27. The 1st circle (black line) and the 20th circle (red line) CVs of complexes **1** (**a**), **2** (**b**) and **3** (**c**).

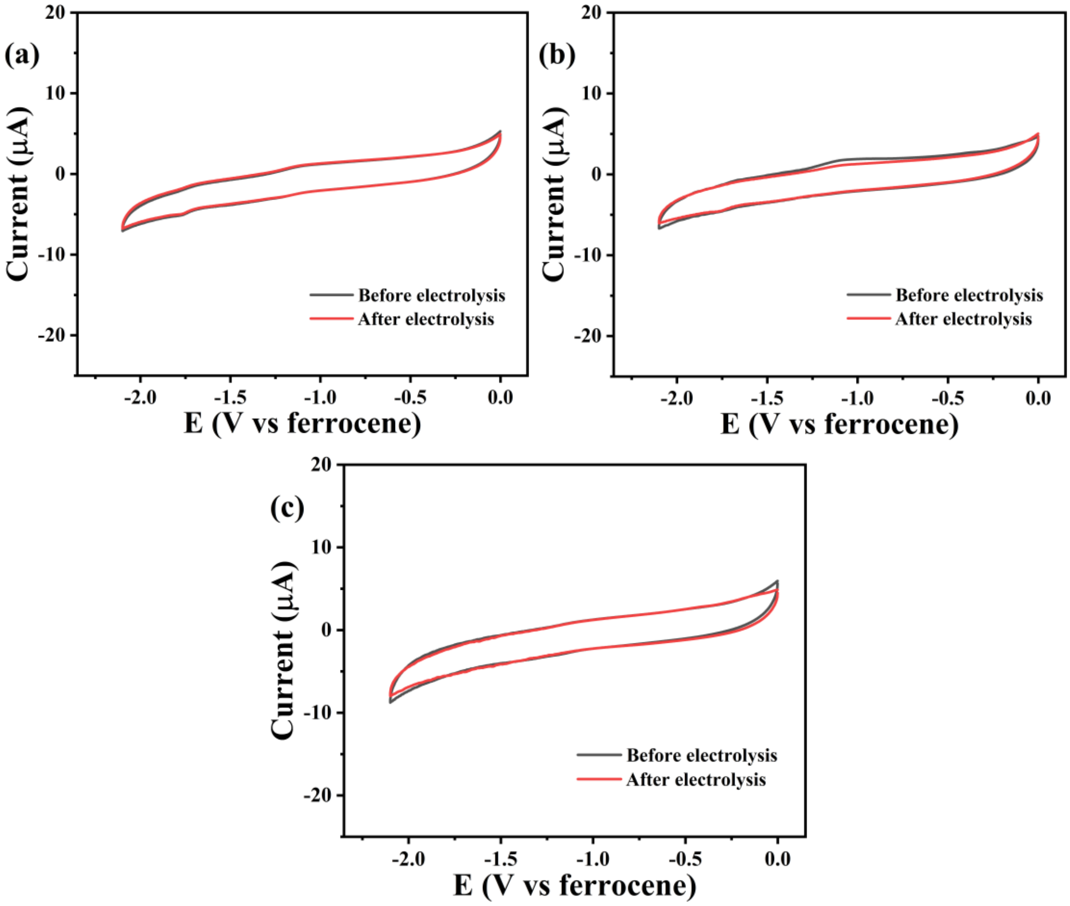

Figure S28. Comparison of CV curves of bare glassy carbon electrodes before and after electrolysis of complexes **1** (**a**), **2** (**b**) and **3** (**c**) in 32 eq. TFA for 1 h.

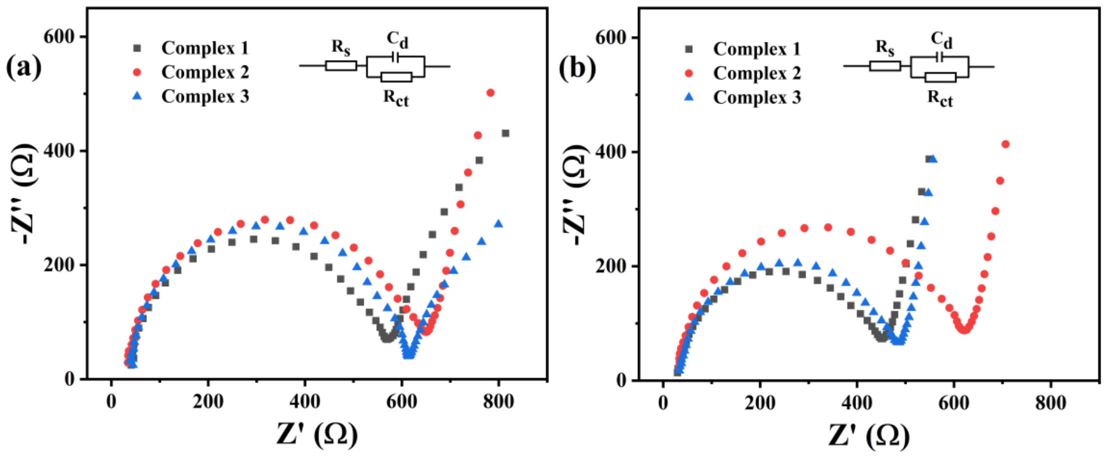

Figure S29. The Nyquist plot of the 0.5 mM complexes **1**-**3** with 32 eq. TFA (**a**), and 32 eq. TsOH (**b**) in DMF.

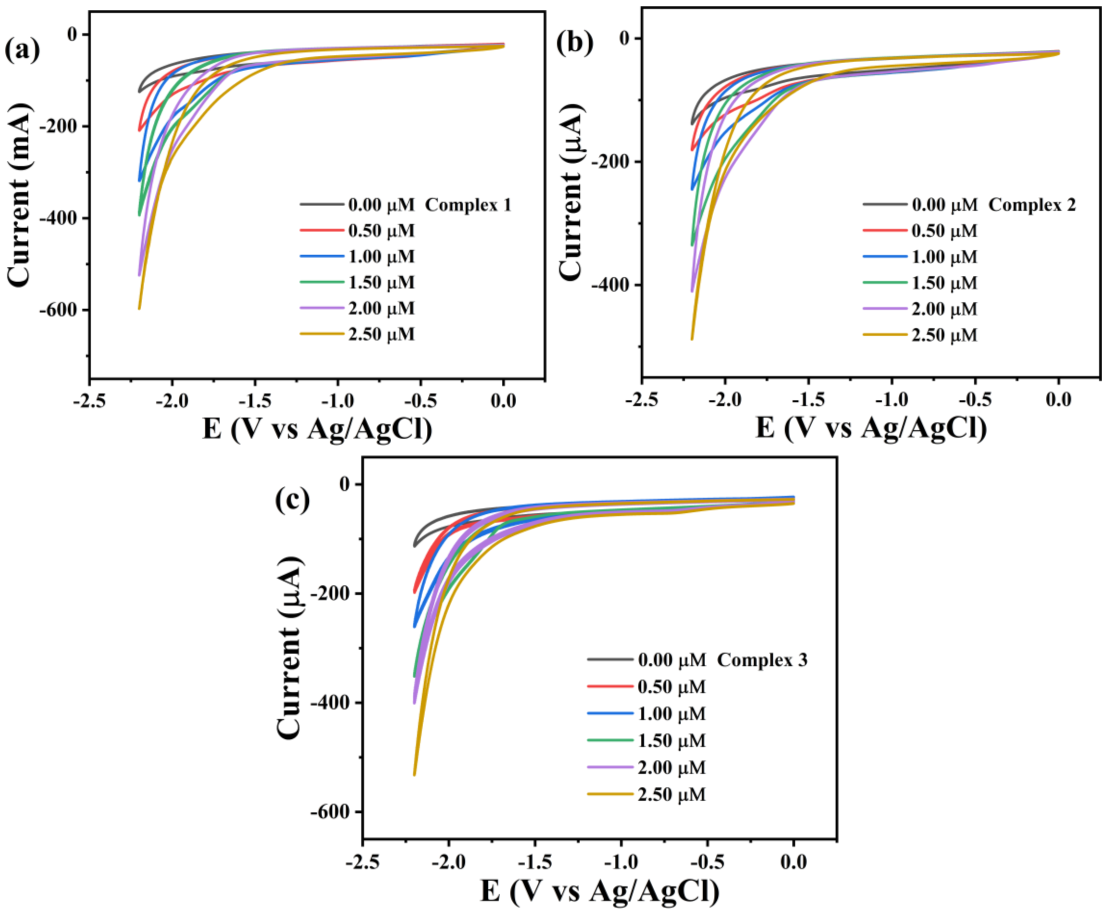

Figure S30. CVs of different concentrations of complexes **1** (**a**), **2** (**b**) and **3** (**c**) in neutral aqueous medium (V_{MeCN}/V_{H2O} = 2/3).

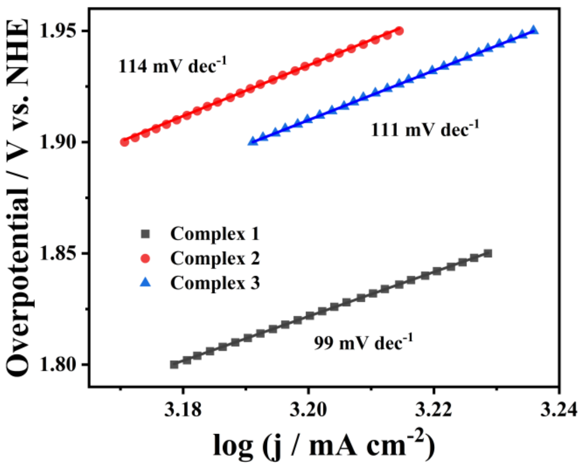

Figure S31. The Tafel slope of the 0.25 μM complexes **1-3** in neutral aqueous medium (V_{MeCN}/V_{H2O} = 2/3).

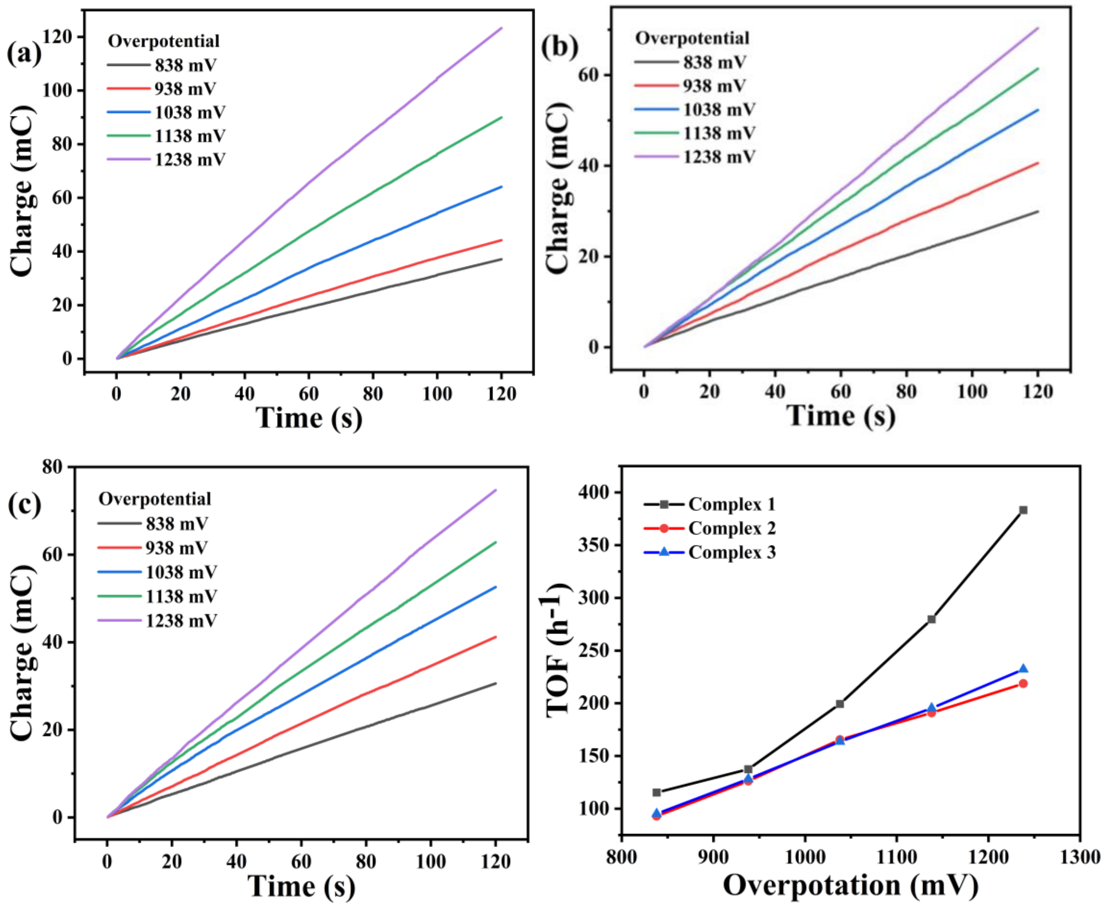

Figure S32. Charges accumulated by electrolysis of 2.5 μM complexes **1** (**a**), **2** (**b**) and **3** (**c**) at different potentials for two minutes and corresponding TOF values (**d**).

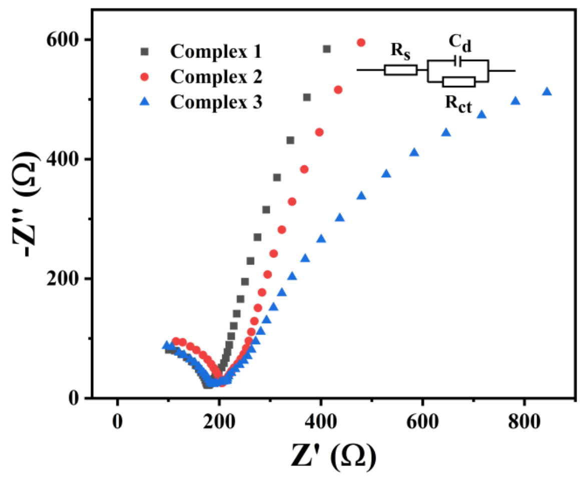

Figure S33. The Nyquist plot of the 0.25 μM complexes **1-3** in neutral aqueous medium (V_{MeCN}/V_{H2O} = 2/3).

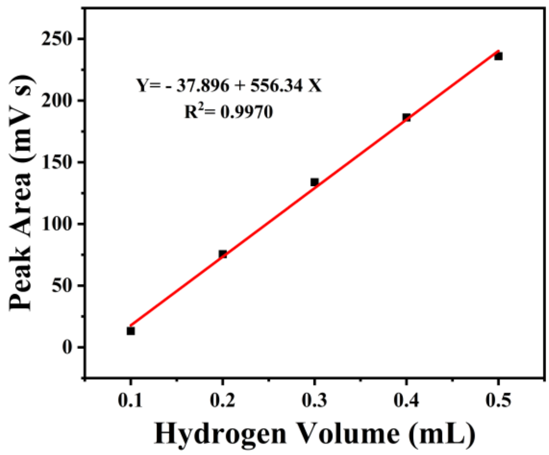

Figure S34. The standard curve of hydrogen volume.

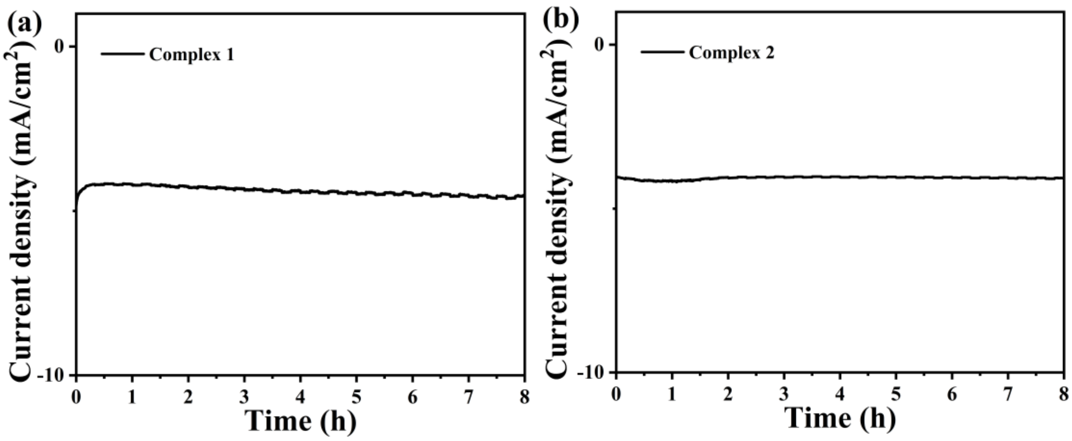

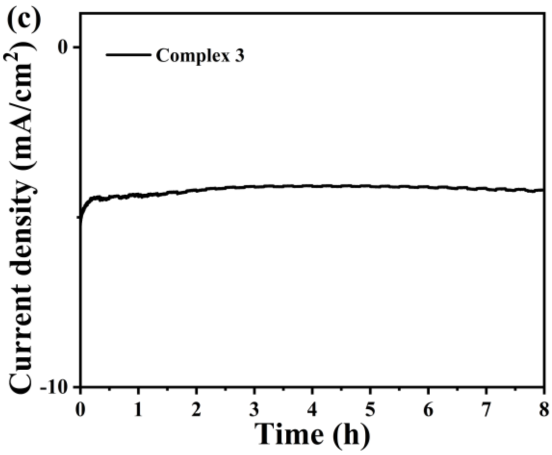

Figure S35. Timed current density measurements of 2.5 μM complexes **1** (**a**), **2** (**b**) and **3** (**c**) electrolyzed at -1.7 V for 8 h in neutral aqueous medium.

Table S1. Crystal data and structure refinement for complex **1**.

Identification code	17linco3_0m_sq
Empirical formula	$C_{55}H_{27}CoF_{10}N_5O_2P$
Formula weight	1069.71
Temperature/K	150
Crystal system	monoclinic
Space group	$P2_1$
a/Å	14.633(3)
b/Å	12.9792(15)
c/Å	27.471(4)
α/°	90
β/°	93.022(7)
γ/°	90
Volume/Å^3	5210.3(14)
Z	4
ρ_{calc}g/cm^3	1.364
μ/mm^{-1}	0.441
F(000)	2160.0
Crystal size/mm^3	0.12 × 0.06 × 0.05
Radiation	MoKα (λ = 0.71073)
2Θ range for data collection/°	3.964 to 52.822
Index ranges	$-15 \le h \le 18$, $-16 \le k \le 14$, $-34 \le l \le 31$
Reflections collected	36187
Independent reflections	18638 [R_{int} = 0.0708, R_{sigma} = 0.1094]
Data/restraints/parameters	18638/1491/1333
Goodness-of-fit on F^2	1.029
Final R indexes [I>=2σ (I)]	R_1 = 0.0916, wR_2 = 0.2350
Final R indexes [all data]	R_1 = 0.1106, wR_2 = 0.2504
Largest diff. peak/hole / e Å^{-3}	1.54/-0.87

Table S2. Crystal data and structure refinement for complex **2**.

Identification code	17jianCo2_0m
Empirical formula	$C_{58}H_{34}CoF_{10}N_5O_2P$
Formula weight	1112.80
Temperature/K	150
Crystal system	triclinic
Space group	P-1
a/Å	8.4217(2)
b/Å	12.1608(2)
c/Å	23.3065(5)
α/°	93.2060(10)
β/°	94.2490(10)
γ/°	94.8940(10)
Volume/Å^3	2367.03(9)
Z	2
ρ_{calc}g/cm^3	1.561
μ/mm^{-1}	3.969
F(000)	1130.0
Crystal size/mm^3	0.16 × 0.08 × 0.06
Radiation	CuKα (λ = 1.54178)
2Θ range for data collection/°	7.31 to 127.592
Index ranges	-9 ≤ h ≤ 9, -14 ≤ k ≤ 13, -27 ≤ l ≤ 27
Reflections collected	28595
Independent reflections	7760 [R_{int} = 0.0818, R_{sigma} = 0.0723]
Data/restraints/parameters	7760/0/695
Goodness-of-fit on F^2	1.064
Final R indexes [I>=2σ (I)]	R_1 = 0.0549, wR_2 = 0.1377
Final R indexes [all data]	R_1 = 0.0643, wR_2 = 0.1461
Largest diff. peak/hole / e Å^{-3}	0.91/-0.64

Table S3. Crystal data and structure refinement for complex **3**.

Identification code	1_sq
Empirical formula	$C_{55}H_{27}CoF_{10}N_5O_2P$
Formula weight	1069.71
Temperature/K	100
Crystal system	monoclinic
Space group	$P2_1/c$
a/Å	14.2487(7)
b/Å	33.8919(17)
c/Å	10.5035(6)
α/°	90
β/°	99.446(4)
γ/°	90
Volume/Å^3	5003.5(5)
Z	4
ρ_{calc}g/cm^3	1.420
μ/mm^{-1}	3.733
F(000)	2160.0
Crystal size/mm^3	0.11 × 0.04 × 0.02
Radiation	CuKα (λ = 1.54178)
2Θ range for data collection/°	5.214 to 127.902
Index ranges	-16 ≤ h ≤ 16, -33 ≤ k ≤ 39, -12 ≤ l ≤ 12
Reflections collected	35205
Independent reflections	8127 [R_{int} = 0.0956, R_{sigma} = 0.0765]
Data/restraints/parameters	8127/0/667
Goodness-of-fit on F^2	1.048
Final R indexes [I>=2σ (I)]	R_1 = 0.0652, wR_2 = 0.1661
Final R indexes [all data]	R_1 = 0.0860, wR_2 = 0.1772
Largest diff. peak/hole / e Å^{-3}	0.54/-0.59

Table S4. Tafel slope in different systems.

System	Tafel slope (mV dec^{-1})		
	2-NBPC-Co (1)	3-NBPC-Co (2)	4-NBPC-Co (3)
DMF (32eq. TFA)	31	49	41
DMF (32eq. TsOH)	34	43	39
buffer (pH=7.0)	99	114	111

Table S5. TOF values at different conditions.

Condition	Overpotential	TOF (h^{-1})		
		2-NBPC-Co (1)	3-NBPC-Co (2)	4-NBPC-Co (3)
DMF	1270	1.87	0.93	1.31
buffer	838	115.32	92.97	95.14
	938	137.40	126.24	128.10
	1038	199.37	165.41	163.55
	1138	279.71	190.91	195.26
	1238	383.25	218.74	232.26

Table S6. Charge transfer resistance (R_{ct}) in different systems.

System	R_{ct} (Ω)		
	2-NBPC-Co (1)	3-NBPC-Co (2)	4-NBPC-Co (3)
DMF (32eq. TFA)	517.1	596.0	560.7
DMF (32eq. TsOH)	407.4	571.0	437.1
buffer (pH=7.0)	159.9	187.8	166.9

Table S7. Comparison of TOF value of cobalt corroles.

Catalysts	TOF(h^{-1})	Overpotential (mV)	proton source/solvent	Refs.
Complex 1	137.4	938	buffer (pH=7.0)	This work
Complex 2	126.2	938	buffer (pH=7.0)	This work
Complex 3	128.1	938	buffer (pH=7.0)	This work
Co_2XBC	85.0	988	buffer (pH=7.0)	[1]
Fe_2XBC	21.6	988	buffer (pH=7.0)	[1]
Mn_2XBC	46.5	988	buffer (pH=7.0)	[1]
CoBPPC	50.0	838	buffer (pH=7.0)	[2]
CoF0	158.6	1088	buffer (pH=7.0)	[3]
PFIC-Co	405	1138	buffer (pH=7.0)	[4]
CoOHC	1447.4	988	buffer (pH=7.0)	[5]
Co-BPNC-PPh_3	450	838	buffer (pH=7.0)	[6]

1. Xu, S.; Cen, J.; Yang, G.; Si, L.; Xiao, X.; Liu, H. Electrocatalytic Hydrogen Evolution by Binuclear Metal (M=Co, Fe, Mn) Xanthine Bridged Bis-corrole. *Chem Res Chin Univ* **2024**. https://doi.org/10.1007/s40242-024-4013-9.
2. Lin, H.; Hossain, M.S.; Zhan, S.; Liu, H.; Si, L. Electrocatalytic hydrogen evolution using triaryl corrole cobalt complex. *Appl Organomet Chem* **2020**, *34*, e5583. https://doi.org/10.1002/aoc.5583.
3. Hao, J.; Liu, Z.; Xu, S.; Si, L.; Wang, L.; Liu, H. Electrocatalytic hydrogen evolution by cobalt(III) triphenyl corrole bearing different number of trifluoromethyl groups. *Inorganica Chim Acta* **2024**, 564. https://doi.org/10.1016/j.ica.2024.121967.
4. Wu, L.; Yao, Y.; Xu, S.; Cao, X.; Ren, Y.; Si, L. et al. Electrocatalytic Hydrogen Evolution of Transition Metal (Fe, Co and Cu)-Corrole Complexes Bearing an Imidazole Group. *Catalysts* **2024**, *14*, 5. https://doi.org/10.3390/catal14010005.
5. Lv, Z.Y.; Yang, G.; Ren, B.P.; Liu, Z.Y.; Zhang, H.; Si, L.P. et al. Electrocatalytic Hydrogen Evolution of the Cobalt Triaryl Corroles Bearing Hydroxyl Groups. *Eur J Inorg Chem* **2023**, *26*, e202200755. https://doi.org/10.1002/ejic.202200755.
6. Xin, X.; Yue, Z.; Gang, Y.; Li-Ping, S.; Hao, Z.; Hai-Yang, L. Electrocatalytic hydrogen evolution of a cobalt A_2B triaryl corrole complex containing –N=PPh_3 group. *Int J Hydrogen Energy* **2022**, *47*, 19062-19072. https://doi.org/10.1016/j.ijhydene.2022.04.104.c

Table S8. Some current values at -2.00 V vs. NHE.

System	Current		
	2-NBPC-Co (1)	**3-NBPC-Co (2)**	**4-NBPC-Co (3)**
DMF (32eq. TFA)	-26.1 μA	-16.14 μA	-19.64 μA
DMF (32eq. TsOH)	-27.49 μA	-17.6 μA	-19.48 μA
buffer (pH=7.0)	-589.3 mA	-479.4 mA	-520.3 mA